Cetyl Trimethyl Ammonium Bromide-Assisted Electrochemical Preparation of Palladium-Nickel Bimetallic Electrode

Zhirong Sun[1], Yanbo Han[1], Ming Gao[1], Xuefeng Wei[1], Xiang Hu[2,]*

[1] College of Environmental & Energy Engineering, Beijing University of Technology, Beijing 100124, P. R. China
[2] College of Chemical Engineering, Beijing University of Chemical Technology, 15 Beisanhuan East Road, Chaoyang District, Beijing 100029, P.R. China
[*]E-mail: huxiang99@163.com

To improve the electrode catalytic activity, palladium-nickel (Pd-Ni) bimetallic electrode was prepared by electrochemical deposition in the presence of cationic surfactant-cetyl trimethyl ammonium bromide (CTAB). Meshed titanium (Ti) was used as substrate. The two electrodes (Pd-Ni/Ti electrode and Pd-Ni(CTAB)/Ti) were characterized by means of cyclic voltammetry (CV), scanning electron microscopy (SEM) and X-ray diffraction (XRD). CV results reveal that the Pd-Ni bimetallic electrode prepared in the presence of CTAB exhibits higher hydrogen adsorption capability than that prepared without CTAB. SEM tests show that CTAB obviously changes the surface morphology of the electrode. Pd-Ni/Ti electrode surface looks like a densely dendritic coating composed of large continuous agglomerates. Pd-Ni(CTAB)/Ti electrode presents clusters of polygonal and loosely packed particles which can increase the surface area and obtain more catalytic sites. XRD results indicate that both the two electrode surface films were made of Pd-Ni bimetals. The quantities of Pd and Ni on Pd-Ni/Ti electrode and on Pd-Ni(CTAB)/Ti electrode were analyzed by inductively coupled plasma-atomic emission spectrometry (ICP-AES). All the experimental results indicate that Pd-Ni(CTAB)/Ti electrode exhibits a favorable surface characteristic and a cheerful prospect of catalytic degradation capability. The reductive dechlorination potential of Pd-Ni(CTAB)/Ti electrode was more higher than that of Pd-Ni/Ti electrode.

1. INTRODUCTION

Halogenated organic compounds are toxic and cause serious environmental challenges because of their widespread use as wood preservatives, pesticides and insulating fluids. They are not

susceptible to bioremediation in respect that high toxicity to microorganism brings low effectiveness [1, 2]. A variety of promising treatment methods have been suggested for the disposal of halogenated organic compounds. These studies include adsorption on granular activated carbon [3], incineration [4], photochemical destruction using UV radiation to cleave C-Cl bonds [5], oxidative processes such as ozonolysis and sonolysis [6], etc. Electrochemical reductive dechlorination is another method employed in recent time with proven capabilities [7-11].

The mechanism of electrochemically reductive dechlorination [12-14] is known as electrocatalytic hydrogenolysis (ECH), a process in which chemisorbed hydrogen atoms generate on the electrode surface by electrolysis of water and then exchange with chlorine atom. As an electrochemical process, ECH is a green technology. The main reductant used in this process-the electron, is a clean agent. Also, it does not produce secondary contaminants which is difficult to be disposed of. The use of ECH for the treatment of wastewater containing halogenated compounds is potentially advantageous compared with traditional techniques such as adsorption on activated carbon or incineration, because adsorption of halogenated compounds on activated carbon simply transfers toxic organic compounds to a different phase; incineration involves high costs and may produce harmful substances such as dioxins.

Among the factors affecting the ECH efficiency, the nature of the electrode material and the feature of the electrode surface are of a prime importance [15]. Palladium (Pd) is considered as the most ideal catalyst for ECH due to its unique function in adsorption of hydrogen [16-19]. There is, however, a particular shortcoming-the high cost of pure Pd cathode catalysts. In order to overcome this shortcoming, the palladium-nickel (Pd-Ni) composite catalytic system was investigated in this paper. Electrochemical deposition is one of the most efficient methods for the growth of metal microparticles [20, 21]. This is a powerful technique for the deposition of many metals since it is rapid and facile, allowing easy control of the nucleation and growth of metal microparticles with different sizes, shapes and distributions [22]. Electrochemical deposition has already been found useful in producing Pd-Ni microparticles on substrates such as titanium (Ti) [23], copper foils [24] and stainless steel [25]. In this work we have developed a method for the preparation of Pd-Ni bimetallic film on meshed Ti in the absence and presence of cetyl trimethyl ammonium bromide (CTAB). The morphology and composition of the fabricated bimetallic film were also discussed in this paper.

2. EXPERIMENTAL SECTION

2.1. Experimental chemicals and materials

Experimental chemicals including acetone, alumina powder, palladium (II) chloride powder, nickel sulfate·$6H_2O$, ammonia, ammonium chloride, sulfuric acid (98%), oxalic acid, sodium carbonate and CTAB were analytic purity and were supplied by Beijing Reagent Co. Meshed Ti was from Anping Wire Screen Mesh Plant, China.

The aperture density and line diameter of meshed Ti were 150 PPI and 0.10 mm, respectively. Solutions were prepared with Millipore-Q water.

2.2. Synthesis of Pd-Ni bimetallic film

Meshed Ti substrate was pretreated prior to electrodeposition. It was put into warm Na_2CO_3 solution for 10 min to degrease, then was placed in boiling oxalic acid solution for 10 min to remove surface native oxides. Finally it was rinsed thoroughly with Millipore-Q water and stored in ethanol for later use. Electrodeposition experiments were performed in a conventional undivided glass cell under galvanostatic condition with agitation of a magnetic stirrer at 100 rpm. A platinum (Pt) foil was used as anode.

To investigate the influence of the surfactant in the synthesis of bimetallic film, Pd-Ni bimetallic electrodes were prepared in the absence and presence of CTAB (Pd-Ni/Ti electrode and Pd-Ni(CTAB)/Ti electrode). The acquired Pd-Ni bimetallic electrodes were washed carefully with distilled water to remove the remaining electrolyte. Pd aqueous solution was prepared by dissolving $PdCl_2$ in 1.2 M HCl solution, and then the nickel salt and ammonium chloride (to increase the conductivity of the bath) were dissolved in Pd aqueous solution to form Pd-Ni bimetallic solution. CTAB was dissolved in water with heating at 30°C and the CTAB solution was added to the bimetallic solution with stirring. Upon mixing, the solution turned turbid because of the formation of CTAB-Pd complex.

A similar phenomenon had been reported by Berhault [26]. This complex was considered to be $[CTA]_2PdBr_4$ which was embedded in CTAB micelles. Then, concentrated ammonia solution was rapidly added with stirring, which was used as a complexer in order to reduce the difference in reduction potentials of the Pd (II) and Ni (II) by reducing the standard redox potential of Pd (II). The whole solution was then maintained in a static state for another 20 min to allow the reaction to proceed sufficiently. Electrodeposition was carried out in above solution to prepare Pd-Ni bimetallic film on meshed Ti substrate with a geometric area of 8 cm^2.

2.3. Characterization of Pd-Ni bimetallic film

All electrochemical analyses were carried out by a Model CHI 660C Potentiostat/Galvanostat controlled by CHI 660C software and a conventional three-electrode system, with a Pt foil as counter electrode and an Hg/Hg_2SO_4-saturated K_2SO_4 as the reference electrode. The working electrode in the electrochemical studies was the as-prepared Pd-Ni/Ti electrode and Pd-Ni(CTAB)/Ti electrode. The electrolytes were 0.5 M H_2SO_4 solution. The Pd-Ni bimetallic film was characterized in terms of morphology, composition and crystal structure. Morphology was observed with a scanning electron microscope (SEM, Hitachi S4700, Japan) at 20.0 kV. The crystal structure of the electrodeposit was analyzed by X-ray diffraction (XRD) using a D8 Discover with Gadds diffractometer with Cu-Kα radiation, operating at 40 kV and 50 mA (Bruker/AXS, Germany). The loading levels of Pd and Ni

particles were analyzed by inductively coupled plasma-atomic emission spectrometry (ICP-AES, RIS Intrepid ER/S, Thermo Elemental, USA).

3. RESULTS AND DISCUSSION

3.1. Preparation of Pd-Ni/Ti electrode

As a heterogeneous catalyst, electrode has evident activation effect on molecules or ions participating in electrochemical reaction [27], which reduces the reaction activation energy greatly. A higher hydrogen adsorption peak current value in CV test is directly related to the larger surface area of the Pd-Ni particles. With larger surface area of Pd-Ni particles, it may offer more chances for the ECH of halogenated organic compounds. Therefore, hydrogen adsorption peak current value was used as reference value to evaluate the catalytic activity of Pd-Ni/Ti electrode.
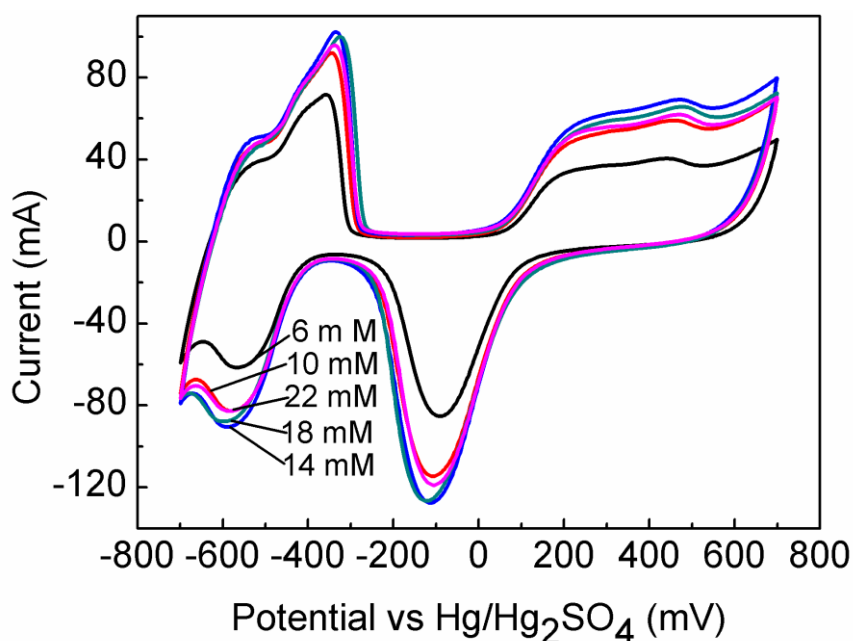
3.1.1. Effect of Pd^{2+} concentration
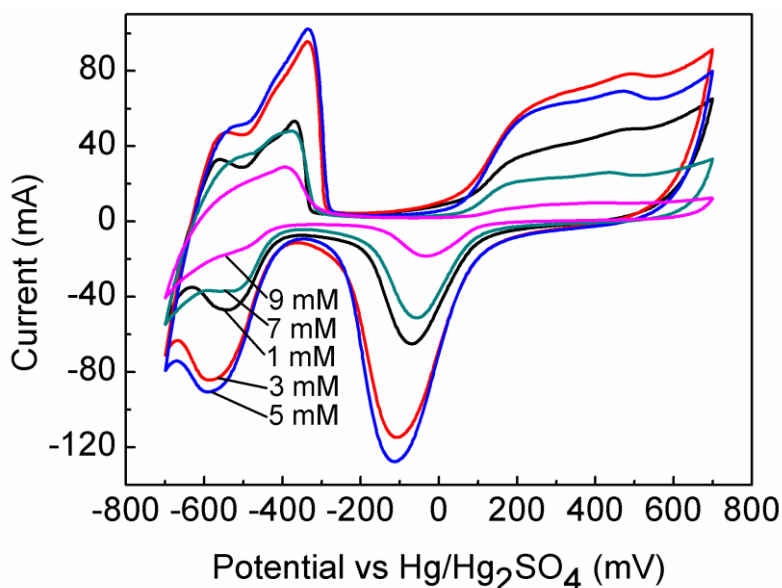
Figure 1. CV curves of Pd-Ni/Ti electrodes prepared at different Pd^{2+} concentrations. Voltage range: -700 mV~700 mV. Scan rate: 50 mV/s. Electrolyte: 0.5 M H_2SO_4 solution

Firstly, Pd^{2+} concentration was investigated under conditions of Ni^{2+} concenteration of 14 mM, initial pH of 6.5, electrodepositing current of 30 mA and electrodepositing time of 50 min. Figure 1 shows the CV curves of the Pd-Ni/Ti electrodes under different Pd^{2+} concentrations (1 mM, 3 mM, 5 mM, 7 mM, and 9 mM, respectively). The concentration of Pd^{2+} determines the amount and the speed of Pd loading. With the increasing of Pd^{2+} concentration, the hydrogen adsorption peak value first increased then decreased after reaching a maximal value. This is consistent with the results from W.

AN et al. [28]. Their studies show that an optimum catalyst loading exists, in terms of the cathode surface area or the percentage of the substrate weight. Therefore, the Pd^{2+} concentration of 5 mM was selected as the constant parameter for electrodepositing of Pd in this study.

3.1.2. Effect of Ni^{2+} concentration

With Pd^{2+} concentration of 5 mM, effect of Ni^{2+} concentration was studied further. Figure 2 shows the CV curves of the Pd-Ni/Ti electrodes under different Ni^{2+} concentrations (6 mM, 10 mM, 14 mM, 18 mM, and 22 mM, respectively) with initial pH of 6.5, electrodepositing current of 30 mA and electrodepositing time of 50 min. With the increasing of Ni^{2+} concentration, the hydrogen adsorption peak value first increased then decreased after reaching a maximal value. This was because that, the deposition speed of Ni was slow and weakened the co-deposition of Pd and Ni when Ni^{2+} concentration was low. On the other hand, Ni^{2+} deposition rate was too fast when Ni^{2+} concentration was too high, leading to the deposition amount of Pd^{2+} shortage, which led to lower hydrogen adsorption peak value. Therefore the Ni^{2+} concentration of 14 mM was selected as the constant parameter for electrodepositing of Ni.
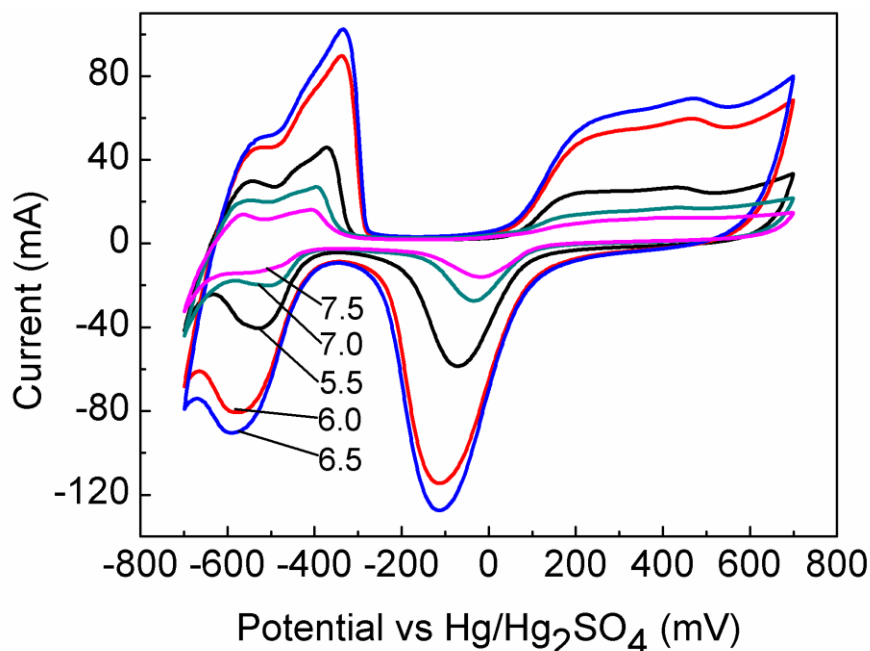

Figure 2. CV curves of Pd-Ni/Ti electrodes prepared at different Ni^{2+} concentrations. Voltage range: -700 mV~700 mV. Scan rate: 50 mV/s. Electrolyte: 0.5 M H_2SO_4 solution.

3.1.3. Effect of initial pH

With Pd^{2+} concentration of 5 mM, Ni^{2+} concentration of 14 mM, electrodepositing current of 30 mA and electrodepositing time of 50 min, the effect of initial pH was investigated further. Figure 3 shows the CV curves of the Pd-Ni/Ti electrodes under different initial pH (5.5, 6.0, 6.5, 7.0, and 7.5,

respectively). It was found that with the increasing of initial pH, the hydrogen adsorption peak value first increased then decreased after reaching a maximal value. When the initial pH was high, Ni content in the Pd-Ni co-deposit decreased, and it was not conducive to the Pd-Ni co-deposition. When the initial pH was low, the precipitate of $Pd(NH_3)_2Cl_2$ might generate, and it was detrimental to the deposition of Pd on the electrode surface. Therefore the initial pH of 6.5 was selected as the constant parameter.
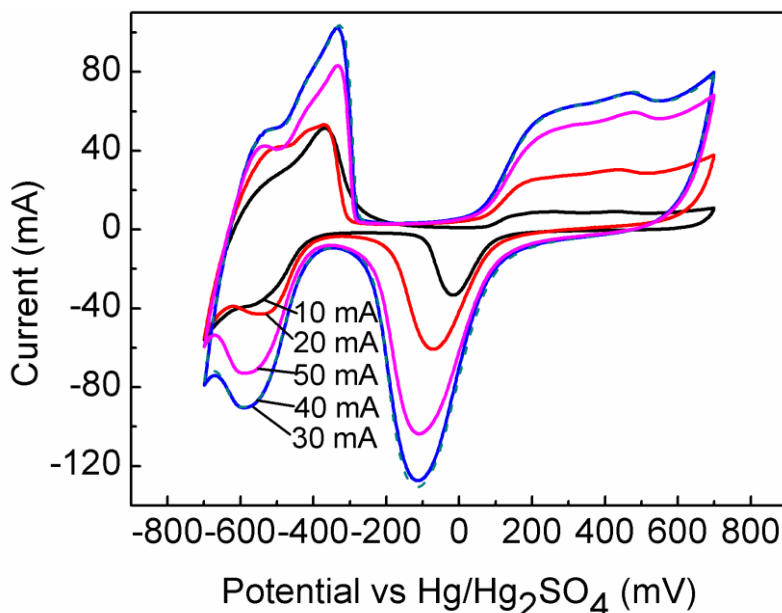

Figure 3. CV curves of Pd-Ni/Ti electrodes prepared at different initial pH. Voltage range: -700 mV~700 mV. Scan rate: 50 mV/s. Electrolyte: 0.5 M H_2SO_4 solution.

3.1.4. Effect of electrodepositing current

With Pd^{2+} concentration of 5 mM, Ni^{2+} concentration of 14 mM, initial pH of 6.5 and electrodepositing time of 50 min, the effect of electrodepositing current was investigated. Figure 4 shows the CV curves of Pd-Ni/Ti electrodes under different electrodepositing currents (10 mA, 20 mA, 30 mA, 40 mA, and 50 mA, respectively).
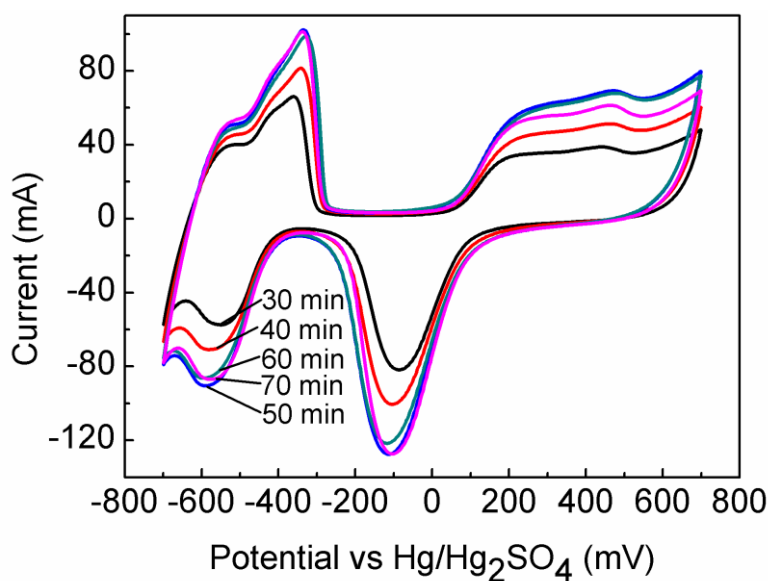
With the increasing of electrodepositing current, the hydrogen adsorption peak first increased then decreased after reaching a maximal value. The hydrogen adsorption peak values were almost equal at the electrodepositing current of 30 mA and 40 mA. This was because that, the loading of Pd-Ni particles on the electrode surface was insufficient when the electrodeposition current was low. On the other hand, Pd-Ni film formed on the electrode surface was too thick and the electrode surface area decreased when the electrodeposition current was too high, which led to the lower hydrogen adsorption peak value. Considering the energy saving, 30 mA was selected as the constant parameter of electrodepositing current.

Figure 4. CV curves of Pd-Ni/Ti electrodes prepared at different electrodepositing currents. Voltage range: -700 mV~700 mV. Scan rate: 50 mV/s. Electrolyte: 0.5 M H_2SO_4 solution.

3.1.5. Effect of electrodepositing time

The effect of electrodepositing time was investigated with Pd^{2+} concentration of 5 mM, Ni^{2+} concentration of 14 mM, initial pH of 6.5 and electrodepositing current of 30 mA. Figure 5 shows the CV curves of Pd-Ni/Ti electrodes under different electrodepositing time (30 min, 40 min, 50 min, 60 min, and 70 min, respectively).
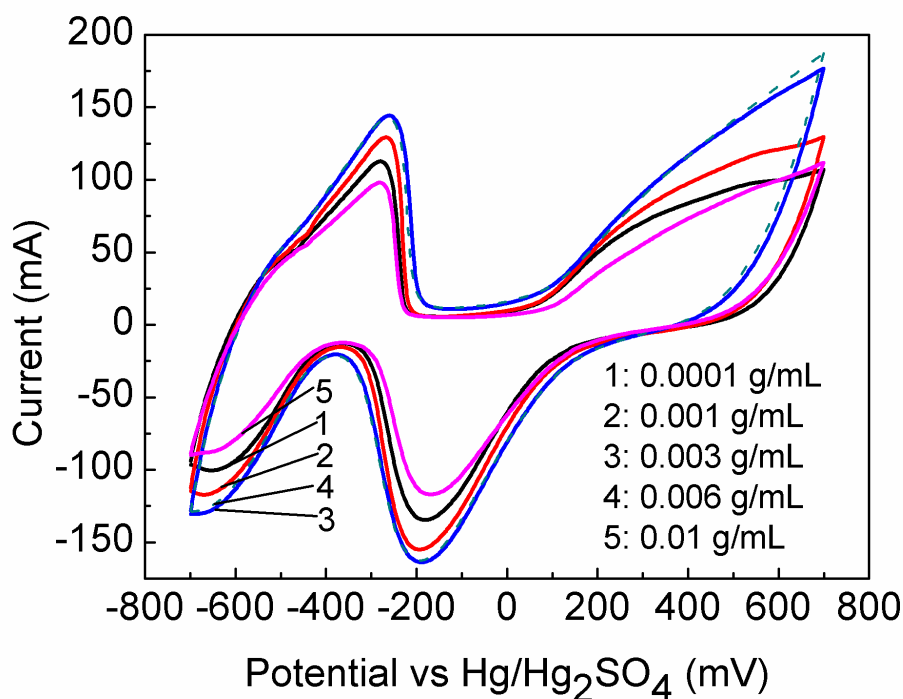

Figure 5. CV curves of Pd-Ni/Ti electrodes prepared at different electrodepositing time. Voltage range: -700 mV~700 mV. Scan rate: 50 mV/s. Electrolyte: 0.5 M H_2SO_4 solution.

It was also found that, with the increasing of electrodepositing time, the hydrogen adsorption peak value first increased then decreased after reaching a maximal value. The maximal hydrogen adsorption peak value was obtained with the electrodepositing time of 50 min. This was because that, when the electrodeposition time was too short, the loading of Pd-Ni particles on the electrode surface was insufficient. When the electrodeposition time was too long, Pd-Ni film formed on the electrode surface was too thick and the electrode surface area decreased, and led to the lower hydrogen adsorption peak value. Therefore, 50 min was selected as the constant parameter of electrodepositing time.

From the results mentioned above, Pd^{2+} concentration of 5mM, Ni^{2+} concentration of 14 mM, initial pH of 6.5, electrodepositing current of 30 mA and electrodepositing time of 50 min could be concluded as the optimum preparation conditions for the Pd-Ni/Ti electrode. The maximal hydrogen adsorption peak value of -90 mA was obtained under these conditions.

3.2. Preparation of Pd-Ni(CTAB)/Ti electrode

To improve the electrocatalytic activity of the electrode, cationic surfactant CTAB was introduced in the preparation of electrode. We synthesized Pd-Ni bimetallic films on meshed Ti substrate under five different CTAB concentrations (0.0001 g/mL, 0.001 g/mL, 0.003 g/mL, 0.006 g/mL, and 0.01 g/mL, respectively), with other factors being kept as the same as that in Pd-Ni/Ti electrode preparation.

Figure 6. CV curves of Pd-Ni(CTAB)/Ti electrodes prepared at different CTAB concentrations. Voltage range: -700 mV~700 mV. Scan rate: 50 mV/s. Electrolyte: 0.5 M H_2SO_4 solution.

Figure 6 shows the CV curves of the Pd-Ni(CTAB)/Ti electrodes prepared at different CTAB concentrations. Because of the adsorption and desorption transition of hydrogen on Pd-Ni particles, evident adsorption peaks were observed around -650 mV. The hydrogen adsorption peak current value increased first with an increasing concentration of CTAB, then decreased after a maximum value of -128 mA was obtained at CTAB concentration of 0.003 g/mL.

It is supposed that the surfactant CTAB plays important roles in at least two aspects. On one hand, it reacts with Pd^{2+} solution to form CTAB-Pd complex. This complex is embedded in CTAB micelles, and then the complex reacts with ammonia and the resultant is not clear yet. We believe that the resultant is generated inside the micelles, which leads to higher stability of the Pd precursor. On the other hand, CTAB can adsorb on the surfaces of these nascent particles to prevent them from forming large agglomerates. Therefore, a favorable electrodeposit can be obtained with the assistance of CTAB.

When CTAB concentration was low, these two effects were not obvious. When CTAB concentration was too high, the excess CTAB could occupy the electrode surface active sites. It was not conducive to the deposition of Pd and led to the lower hydrogen adsorption peak value. Therefore, CTAB concentration of 0.003 g/mL was selected as the constant parameter for preparation of Pd-Ni(CTAB)/Ti electrode.

3.3. Crystal structure characterization of the Pd-Ni bimetallic film

The crystal structures of the prepared Pd-Ni films were examined by XRD.
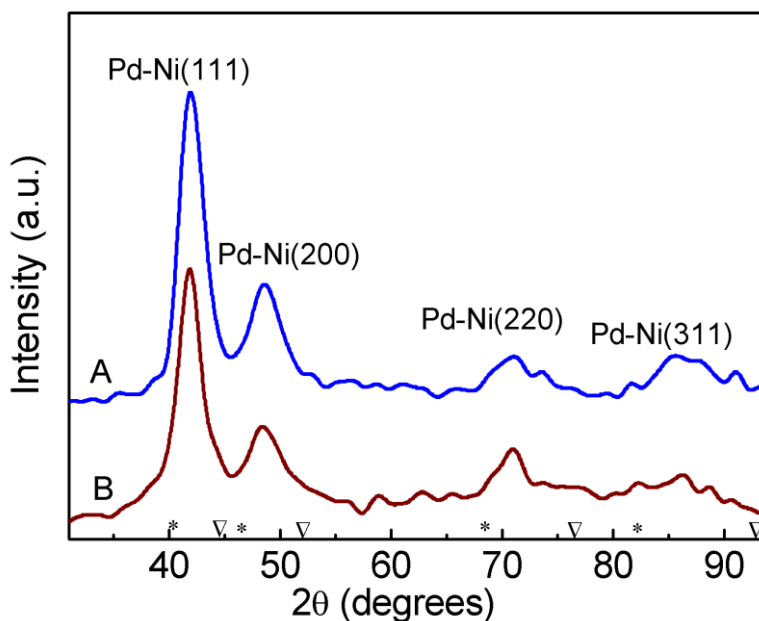
Figure 7. XRD pattern of Pd-Ni bimetallic films prepared in the absence (A) and presence (B) of CTAB; standard position: * Pd, ▽ Ni.

Figure 7 shows the XRD results of Pd-Ni films formed in the absence and presence of CTAB. Both samples display the (111), (200), (220) and (311) reflection characteristic of the face-centered cubic (FCC) crystal structure. As for the characteristic peaks of the (111) plane, the d-spacing values for Pd-Ni films formed in the absence and presence of CTAB are 2.17613 Å and 2.15709 Å, lie in between those of pure Pd (JCPDS 5-681, 2.24600 Å) and Ni (JCPDS 4-850, 2.03400 Å). The (200), (220) and (311) planes also show the same trends, confirming that the films are made of Pd-Ni bimetals.

3.4. Cyclic voltammetry

Figure 8 shows the CV curves of Pd-Ni/Ti electrode and Pd-Ni(CTAB)/Ti electrode prepared at optimum conditions, separately. As shown in Figure 8, the hydrogen adsorption peak value of Pd-Ni(CTAB)/Ti electrode (curve B) was larger than that of Pd-Ni/Ti electrode (curve A). The former got maximal hydrogen adsorption peak value of -128 mA around -650 mV, which was 38 mA larger than the later, -90 mA. The remarkably high hydrogen adsorption peak value could be attributed to the high active surface area of Pd-Ni particles with presence of CTAB. Because of the poor symmetry of the hydrogen adsorption peak, the reduction charge of surface oxide formed over the top layer of the Pd-Ni particles during the anodic scan was used in calculating the active surface area. This method has been used to determine the active surface area of pure Pd electrodes and Pd-based alloy electrodes [29, 30]. A value of 405 $\mu C/cm^2$ was considered to correspond to the reduction of a monolayer of surface oxide [31]. By calculation using this method, the active surface area of Pd-Ni bimetallic film prepared in the presence of CTAB is 2.06×10^3 cm^2 against 1.29×10^3 cm^2 without CTAB.
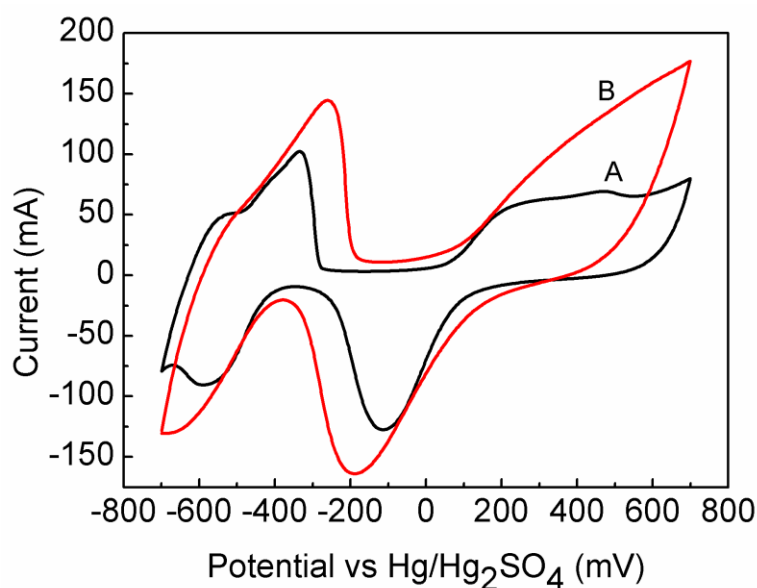
Figure 8. CV curves of Pd-Ni/Ti electrode (A) and Pd-Ni(CTAB)/Ti electrode (B). Voltage range: -700 mV~700 mV. Scan rate: 50 mV/s. Electrolyte: 0.5 M H_2SO_4 solution.

3.5. Morphology characterization of the Pd-Ni bimetallic film
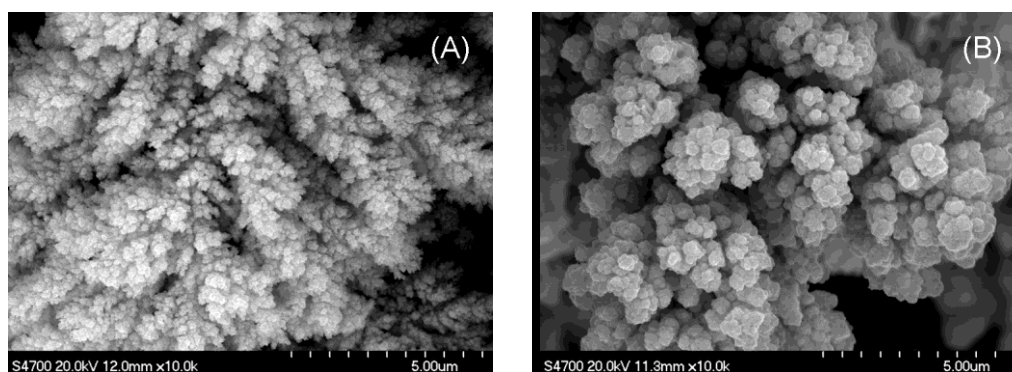
Figure 9. SEM images of Pd-Ni/Ti electrode (A) and Pd-Ni(CTAB)/Ti electrode (B).

Figure 9 shows the morphologies of Pd-Ni bimetallic films formed in the absence and presence of CTAB, respectively. Without CTAB a densely dendritic coating composed of large continuous agglomerates was obtained (Figure 9 (A)). All of the Pd-Ni grains were in close contact with each other. Figure 9 (B) shows the morphology of Pd-Ni bimetallic film in the presence of CTAB. The bimetallic film presented clusters of polygonal and loosely packed particles. This configuration could increase the surface area and supply more catalytic sites. The catalyst structural features shown in Figure 9 (B) have a profound effect on the activity of the Pd-Ni film as revealed by the CV curves (Figure 8). This could be attributed to the higher active surface area.

3.6. Composition of the Pd-Ni bimetallic film

The loading levels of Pd and Ni particles on Pd-Ni/Ti and Pd-Ni (CTAB)/Ti electrodes were analyzed by ICP-AES. The loadings of Pd and Ni on Pd-Ni/Ti electrode were 2.06 mg/cm^2 and 1.35 mg/cm^2, respectively. Those on the Pd-Ni(CTAB)/Ti electrode were 2.21 mg/cm^2 and 1.36 mg/cm^2, respectively. The addition of CTAB slightly increased the loading amounts of Pd and Ni, but the electrocatalytic activity was improved obviously. The enhancement of the electrode surface catalytic activity is attractive for application in electrochemical dechlorination.

4. CONCLUSIONS

Pd-Ni bimetallic film with high electrocatalytic activity was prepared on Ti substrate under modification of CTAB. The preparation conditions of the Pd-Ni(CTAB)/Ti electrode are Pd^{2+} concentration of 5 mM, Ni^{2+} concentration of 14 mM, initial pH of 6.5, electrodepositing current of 30 mA, electrodepositing time of 50 min, and CTAB concentration of 0.003 g/mL, respectively. The electrode surface film is made of Pd-Ni bimetals with FCC structure. CV results indicate that the activity of the electrode prepared with CTAB is much higher than that without CTAB. The addition of CTAB modifies the morphology of Pd-Ni bimetallic film, increases the surface area and supplies more catalytic sites.

The surfactant CTAB has important effects on the hydrogen adsorption capability of the bimetallic film. The improvement could be attributed to the increasing of high active surface area due to the modification of CTAB. Compared with Pd-Ni/Ti electrode, the Pd-Ni(CTAB)/Ti electrode shows favorable surface characteristics and promising capability for electrochemically reductive dechlorination.

References

1. Q. Liu, Y. Chen, J.D. Wang, J.M Yu, J.M. Chen and G.D Zhou, *Int. J. Electrochem. Sci.*, 6 (2011) 2366
2. T. Zhou, Y.Z. Li and T.T. Lim, *Sep. Purif. Technol.*, 76 (2010) 206
3. S.P. Pajooheshfar and M. Saeedi, *Water Environ. Res.*, 81 (2009) 641
4. T. Kishi, S. Suzuki, M. Takagi, T. Kawakami and S. Onodera, *Chemosphere*, 76 (2009) 205
5. S.G. Poulopoulos, M. Nikolaki, D. Karampetsos and C.J. Philippopoulos, *J. Hazard. Mater.*, 153 (2008) 582
6. Z.Z. Shen, J.Z. Cheng and S.J. Wu, *J. Environ. Sci.*, 16 (2004) 431
7. L. Liu, G.H. Zhao, M.F. Wu, Y.Z. Lei and R. Geng, *J. Hazard. Mater.*, 168 (2009) 179
8. B. Yang, G. Yu and J. Huang, *Acta Phys.-Chim. Sin.*, 22 (2006) 306
9. C.Y. Cui, X. Quan, H.T. Yu and Y.H. Han, *Appl. Catal., B*, 80 (2008) 122
10. H. Cheng, K. Scott and P.A. Christensen, *J. Electrochem.* Soc., 150 (2003) D17
11. C. Durante, A.A. Isse, G. Sandina and A. Gennaro, *Appl. Catal., B*, 88 (2009) 479
12. B. Yang, G. Yu and J. Huang, *Environ. Sci. Technol.*, 41 (2007) 7503
13. I.F. Cheng, Q. Fernando and N. Korte, *Environ. Sci. Technol.*, 31 (1997) 1074
14. Z.Q. He, Q. Wang, J.J. Sun, J.M. Chen and S. Song, *Int. J. Electrochem. Sci.*, 6 (2011) 2932
15. P. Dabo, A. Cyr, F. Laplante, F. Jean, H. Menard and J. Lessard, *Environ. Sci. Technol.*, 34 (2000) 1265
16. J.L. Han, W.Y. Hu and H.Q. Deng, *Surf. Interface Anal.*, 41 (2009) 590
17. M. Zhang, F.L. Cheng, Z.Q. Cai and H.J. Yao, *Int. J. Electrochem. Sci.*, 5 (2010) 1026
18. L.L. Jewell and B.H. Davis, *Appl. Catal., A*, 310 (2006) 1
19. V.K. Potapov, V.M. Matyuk, A.S. Baturin and L.I. Trakhtenberg, *Russ. J. Phys. Chem.* A, 82 (2008) 1415
20. A.D. Bani-Yaseen, *Int. J. Electrochem. Sci.*, 5 (2010) 1837
21. G. Saravanan and S. Mohan, *Int. J. Electrochem. Sci.*, 6 (2011) 1468
22. C.W. Welch and R.G. Compton, *Anal. Bioanal. Chem.*, 384 (2006) 601
23. K.S. Kumar, P. Haridoss and S.K. Seshadri, *Surf. Coat. Technol.*, 202 (2008) 1764
24. T. Shobha, C.L. Aravinda, P. Bera, L.G. Devi and S.M. Mayanna, *Mater. Chem. Phys.*, 80 (2003) 656
25. S.E. Nam and K.H. Lee, *J. Membr. Sci.*, 170 (2000) 91
26. G. Berhault, M. Bausach, L. Bisson, L. Becerra, C. Thomazeau and D. Uzio, *J. Phys. Chem. C*, 111 (2007) 5915
27. S. Rondinini and A. Vertova, *Electrochim. Acta*, 49 (2004) 4035
28. W. An, J.K. Hong and P.N. Pintauro, *J. Appl. Electrochem.*, 28 (1998) 947

29. R. Pattabiraman, *Appl. Catal., A*, 153 (1997) 9
30. A.N. Correia, L.H. Mascaro, S.A.S. Machado and L.A. Avaca, *Electrochim. Acta*, 42 (1997) 493
31. T. Chierchie, C. Mayer and W.J. Lorenz, *J. Electroanal. Chem.*, 135 (1982) 211